Monthly Notices
of the
ROYAL ASTRONOMICAL SOCIETY

MNRAS **504,** L45–L50 (2021)
Advance Access publication 2021 April 16

doi:10.1093/mnrasl/slab037

A transit timing variation observed for the long-period extremely low-density exoplanet HIP 41378 f

Edward M. Bryant [1,2]★ Daniel Bayliss [1,2] Alexandre Santerne [3] Peter J. Wheatley [1,2] Valerio Nascimbeni [4] Elsa Ducrot,[5] Artem Burdanov,[5,6] Jack S. Acton,[7] Douglas R. Alves [8] David R. Anderson [1,2] David J. Armstrong [1,2] Supachai Awiphan,[9] Benjamin F. Cooke [1,2] Matthew R. Burleigh [7] Sarah L. Casewell,[7] Laetitia Delrez,[5,10,11] Brice-Olivier Demory,[12] Philipp Eigmüller,[13] Akihiko Fukui,[14,15] Tianjun Gan [16] Samuel Gill,[1,2] Michael Gillon,[17] Michael R. Goad,[7] Thiam-Guan Tan [18] Maximilian N. Günther [19]† Bronwen Hardee [20] Beth A. Henderson,[7] Emmanuel Jehin,[10] James S. Jenkins [8,21] Molly Kosiarek [22]‡ Monika Lendl [11] Maximiliano Moyano [23] Catriona A. Murray [24] Norio Narita,[15,25,26,27] Prajwal Niraula [6] Caroline E. Odden,[28] Enric Palle,[15,29] Hannu Parviainen,[15,29] Peter P. Pedersen [24] Francisco J. Pozuelos [17,10] Benjamin V. Rackham [6]§ Daniel Sebastian [30] Chris Stockdale [31] Rosanna H. Tilbrook,[7] Samantha J. Thompson [24] Amaury H.M.J. Triaud [30] Stéphane Udry,[11] Jose I. Vines, Richard G. West [1,2] and Julien de Wit[6]

Affiliations are listed at the end of the paper

Accepted 2021 April 2. Received 2021 March 31; in original form 2021 March 10

ABSTRACT

HIP 41378 f is a temperate $9.2 \pm 0.1\,R_\oplus$ planet with period of 542.08 d and an extremely low density of $0.09 \pm 0.02\,\mathrm{g\,cm^{-3}}$. It transits the bright star HIP 41378 ($V = 8.93$), making it an exciting target for atmospheric characterization including transmission spectroscopy. HIP 41378 was monitored photometrically between the dates of 2019 November 19 and 28. We detected a transit of HIP 41378 f with NGTS, just the third transit ever detected for this planet, which confirms the orbital period. This is also the first ground-based detection of a transit of HIP 41378 f. Additional ground-based photometry was also obtained and used to constrain the time of the transit. The transit was measured to occur 1.50 h earlier than predicted. We use an analytic transit timing variation (TTV) model to show the observed TTV can be explained by interactions between HIP 41378 e and HIP 41378 f. Using our TTV model, we predict the epochs of future transits of HIP 41378 f, with derived transit centres of $T_{\mathrm{C},4} = 2459\,355.087^{+0.031}_{-0.022}$ (2021 May) and $T_{\mathrm{C},5} = 2459\,897.078^{+0.114}_{-0.060}$ (2022 November).

Key words: techniques: photometric – planets and satellites: detection – planets and satellites: individual: HIP 41378 f – stars: individual: HIP 41378.

1 INTRODUCTION

The bright ($V = 8.93$) F-type star HIP 41378 is known to host five transiting planets (Vanderburg et al. 2016), based on photometric data taken during campaign C5 of the *K2* mission (Howell et al. 2014). The outer most planet known in the system, HIP 41378 f only transited once during these observations. A second transit of HIP 41378 f was observed during *K2* campaign C18 and showed it to have a maximum possible orbital period of 1084.159 d (Becker et al. 2019). Extensive spectroscopic monitoring with HARPS by Santerne et al. (2019) revealed the true period of HIP 41378 f to be 542.08 d – half the possible maximum.

With a mass of $M_\mathrm{p} = 12 \pm 3\,\mathrm{M}_\oplus$ and a radius of $R_\mathrm{p} = 9.2 \pm 0.1 R_\oplus$, the low density of HIP 41378 f, combined with its cool temperature, makes it a particularly interesting target for atmospheric characterization. Using the system parameters from Santerne et al. (2019), we calculate a Transmission Spectroscopy Metric (TSM) for HIP 41378 f of 343 (Kempton et al. 2018), which shows HIP 41378 f to be very well suited to transmission spectroscopy follow-up. For these observations, a precise orbital ephemeris is needed. Despite the high-quality *K2* data, with only two recorded transits, there was previously no information regarding any transit timing variations (TTVs) of HIP 41378 f. In a multiplanet system, a planet with a long orbital period such as HIP 41378 f may experience large TTVs (e.g. Agol et al. 2005; Kawahara & Masuda 2019). Since HIP 41378 f resides in near 2:1 and 3:2 mean motion resonances with planet e

★ E-mail: Edward.bryant@warwick.ac.uk
† Juan Carlos Torres Fellow.
‡ NSF Graduate Research Fellow.
§ 51 Pegasi b Fellow.

© 2021 The Author(s).
Published by Oxford University Press on behalf of Royal Astronomical Society. This is an Open Access article distributed under the terms of the Creative Commons Attribution License (http://creativecommons.org/licenses/by/4.0/), which permits unrestricted reuse, distribution, and reproduction in any medium, provided the original work is properly cited.

Downloaded from https://academic.oup.com/mnrasl/article/504/1/L45/6228864 by guest on 11 December 2024

and d respectively, we may expect TTVs on the order of hours to days.

Ground-based photometric observations of the HIP 41378 system are needed to measure any TTVs to place additional constraints on the masses and orbital periods of planets in the HIP 41378 system. Monitoring the TTVs also has the potential to reveal other exoplanets in the system, and additionally will help predict future transit events for atmospheric characterization. However, for a star with a magnitude of $V = 8.93$, the field of view of most ground-based photometric facilities will often not include enough comparison stars of a similar brightness (Collins et al. 2018). In fact, for HIP 41378, the nearest star with a *Gaia G* magnitude difference of less than 0.5 mag is 17 arcmin away (Gaia Collaboration et al. 2018).

2 PHOTOMETRIC OBSERVATIONS

2.1 NGTS

The Next Generation Transit Survey (NGTS; Wheatley et al. 2018) is a photometric facility situated at ESO's Paranal Observatory in Chile. It consists of 12 fully-robotic telescopes with 20-cm diameter apertures and wide fields of view of 8 deg^2. The dominant photometric noise sources in NGTS bright star light curves have been shown to be Gaussian and uncorrelated between the individual telescopes (Bryant et al. 2020). Combined with the wide field of view, this allows NGTS to use simultaneous observations with multiple telescopes to achieve high-precision light curves of bright stars (Bryant et al. 2020; Smith et al. 2020)

HIP 41378 was observed with NGTS on the nights UT 2019 November 19, 24, and 25. On all nights, HIP 41378 was monitored using eleven NGTS telescopes, each using the custom NGTS filter (520–890 nm) and an exposure time of 10 s. Across all nights, a total of 23 841 images were taken. The target was above an altitude of 30° for all the observations, and the observing conditions were good.

The NGTS data were reduced using a custom aperture photometry pipeline, which utilizes the SEP PYTHON library (Bertin & Arnouts 1996; Barbary 2016). The pipeline uses the *Gaia* DR2 catalogue (Gaia Collaboration et al. 2016, 2018) to automatically identify comparison stars that are similar in magnitude, colour, and CCD position to HIP 41378 (for more details, see Bryant et al. 2020). Comparison stars that a shown to display variability or high levels of photometric scatter are excluded from the reduction. The NGTS photometry is plotted in Fig. 1.

2.2 SPECULOOS

HIP 41378 was observed by SPECULOOS (Search for habitable Planets EClipsing ULtra-cOOl Stars; Burdanov et al. 2018; Delrez et al. 2018; Gillon 2018; Sebastian et al. 2021). It was observed from the SPECULOOS Southern Observatory (SSO) at Paranal, Chile on UT 2019 November 24 and from the SPECULOOS Northern Observatory (SNO) at the Teide Observatory on Tenerife, Spain, on UT 2019 November 25. The SSO observations consists of 342 images obtained using the r' filter, an exposure time of 12 s, and a defocus of 300 steps to avoid saturation. SNO obtained 254 images using also the r' filter, with an exposure time of 12 and a defocus of 300 steps. For each night of observation, the automatic SSO Pipeline (Murray et al. 2020) was used to reduce images and extract precise photometry. The SSO Pipeline is built upon the CASUTOOLS software (Irwin et al. 2004) and performs automated differential photometry to mitigate ground-based systematics, including a correction for time-

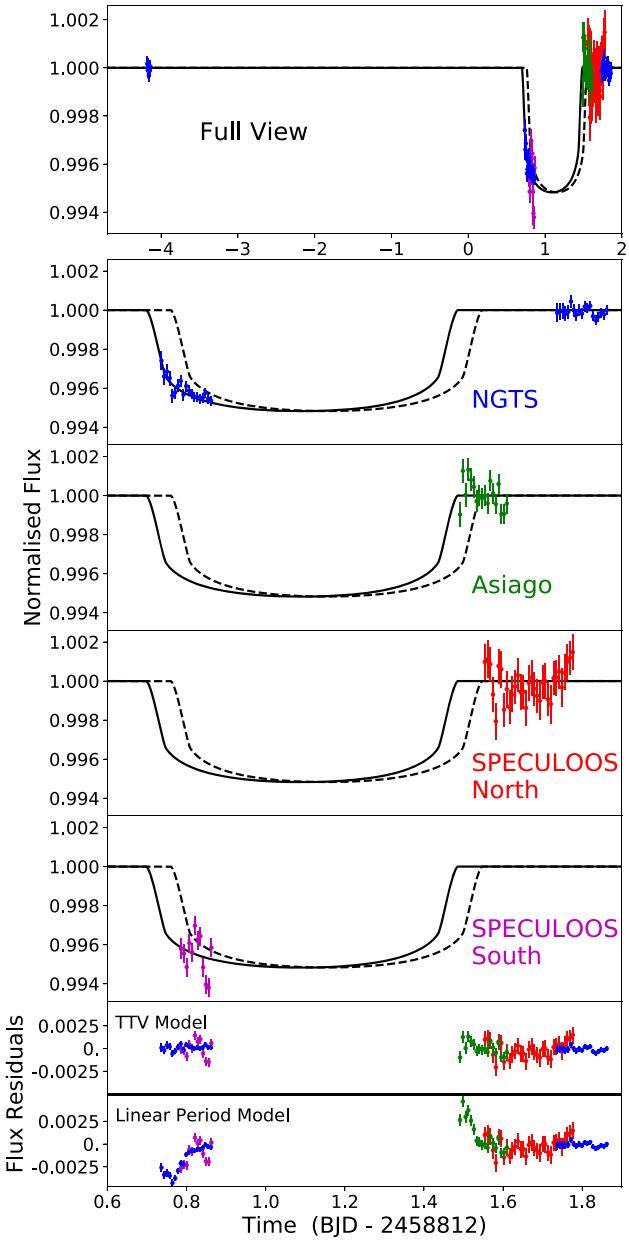


Figure 1. Ground-based relative time-series photometry of HIP 41378. All the photometric data included in the analysis are shown in the top panel. The individual data sets are presented in the following panels: NGTS (blue; second panel) showing a zoom-in on the transit of HIP 41378 f, ASIAGO (green; third panel), SNO (red; fourth panel), and SSO (magenta; fifth panel). All data are binned to 10 min. The predicted transit model of HIP 41378 f from the *K2* and HARPS data is given by the dashed black line, and the model from our sampling process is given by the solid black line. The residuals to the TTV model from our fitting are presented in the sixth panel, and the residuals to the predicted linear period model from the two prior transits are presented in the bottom panel. We note that the colours used to denote the individual data sets are consistent across each panel. Note that we plot the detrended NGTS data and the relative flux offsets between the photometry obtained at different facilities were fit as free parameters during the modelling set out in Section 3.

Downloaded from https://academic.oup.com/mnrasl/article/504/1/L45/6228864 by guest on 11 December 2024

varying telluric water vapour. The SNO and SSO data are plotted in Fig. 1.

2.3 Asiago telescope

HIP 41378 was observed on the night UT 2019 November 25 using the 67/92-cm Schmidt telescope based at the Asiago Observatory in northern Italy, operated by the Italian National Institute of Astrophysics (INAF). A total of 301 images were obtained through the Sloan *r* filter under a good sky quality, using a constant exposure time of 30 s and defocusing the camera to minimize pixel-to-pixel systematic errors. The light curve was extracted by using a custom version of the STARSKY code, a pipeline to perform high-precision differential photometry originally developed for the TASTE project (Nascimbeni et al. 2011). The unbinned RMS is 2.0 mmag, the scatter being much larger at the beginning of the series due to the much higher airmass (1.97 for the first frame). All the time stamps were converted to the BJD-TDB system (Eastman, Siverd & Gaudi 2010). The Asiago data, binned over a 10-min time-scale (rms: 825 ppm), are plotted in Fig. 1 (green points). The Asiago data are plotted in Fig. 1.

2.4 Photometric transit detection

The NGTS data show a clear flux decrease, which is consistent to the predicted transit depth and near to the predicted transit time. This flux decrease is clearly seen in the top two panels of Fig. 1. We note that the NGTS photometry is of sufficient precision that an ingress occurring at the time predicted from the *K2* and HARPS data would be robustly detected. The SSO and Asiago data are consistent with the change in transit time seen by NGTS, ruling out an on-time ingress and egress, respectively. The SNO data rule out a late transit. With photometric coverage on three separate nights surrounding the transit event, we are confident that the flux offset seen in the NGTS data is a real signal. However, the relative flux offsets between the data from the different facilities, including the offset of the SSO data, were fit independently as free parameters during the modelling detailed in Section 3. The combination of these four data sets gives us confidence that the transit occurred earlier than the prediction from the linear orbital ephemeris derived from the *K2* and HARPS data (Santerne et al. 2019). This is the third transit of this planet to be detected and the first from the ground, with the other two being detected from data obtained by the *K2* mission. The detection of this transit confirms the 542.08-d period predicted for this planet from *K2* and HARPS data (Santerne et al. 2019).

2.5 Additional ground-based photometry

Additional photometry for HIP 41378 was also obtained with various other ground-based facilities: PEST, LCO (CTIO), PROMPT-8 (CTIO), MUSCAT2 at Teide Observatory, Lick Observatory, Hazelwood Observatory, and Phillip's Academy Observatory. Unfortunately, due to poor observing conditions or a lack of suitable comparison stars, none of the data from these facilities had a photometric precision better than a threshold of 2 ppt per 10 min. As such we do not include these data sets in our analysis.

3 ANALYSIS

We jointly modelled the photometry from NGTS, ASIAGO, SSO, and SNO in order to determine the time of transit centre for the 2019 November transit, $T_{C,3}$. Note we use the notation $T_{C,N}$ to refer

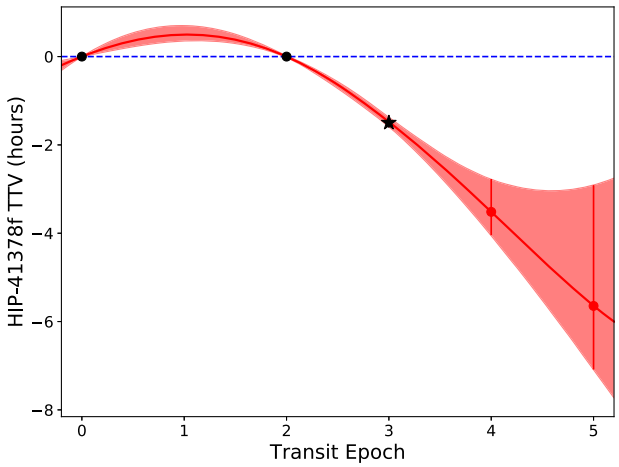


Figure 2. Transit times for HIP 41378 f. The black points give the T_C values for the two transits of HIP 41378 f observed by *K2*. The black star gives the new $T_{C,3}$ determined in this work. The 1σ error bars on these values are plotted but are two small to be visible. The red points and error bars give the predicted transit times for $T_{C,4}$ (2021 May) and $T_{C,5}$ (2022 November) and their respective 1σ uncertainties. The solid red line gives the median TTV signal from the TTV analysis (see Section 4), and the red shaded area gives the 1σ uncertainty on this signal. The TTV values are relative to the linear ephemeris based on the period from Santerne et al. (2019) of $T_0 = 2457\,186.914\,51$ and $P_f = 542.079\,75$ d, and this linear ephemeris is shown by the blue dashed line.

to the time of transit centre for transit epoch *N*. The first transit of HIP 41378 f in *K2* C5 is taken to occur at $T_{C,0}$. We generated a transit light-curve template based on the parameters from Vanderburg et al. (2016), and using the period derived by Santerne et al. (2019). We performed an MCMC sampling process to model the ground-based photometric data. The free parameters used in the modelling were $T_{C,3}$, the limb-darkening coefficients, the detrending coefficients for the NGTS data, and relative flux offset factors for the other data sets. Note that each NGTS single-telescope light curve was detrended against airmass independently from the other telescopes, and a single linear trend with time is applied to the entire NGTS multitelescope light curve. We used a quadratic limb-darkening profile, constraining the coefficients based on theoretically derived limb-darkening coefficients for the NGTS filter. The *r*' filter used for the SSO observations has a large amount of overlap with the wavelength range of the NGTS filter, and so the limb-darkening coefficients derived for the NGTS filter provide a good approximation for the SSO data. The precision of the SSO data also means that including an additional set of limb-darkening coefficients for the SSO data does not have an effect on the derived value of $T_{C,3}$. Therefore, we use the theoretical values of 0.315 ± 0.004 and 0.289 ± 0.001, which were computed from the Claret & Bloemen (2011) tables, as Gaussian priors for the model for all data sets.

The sampling was performed using the Ensemble Sampler from EMCEE (Foreman-Mackey et al. 2013). We ran 70 chains for 10 000 steps, following a burn-in phase of 2500 steps. The number of effective samples for each parameter ranged from 600 000 to 800 000, with the number of effective samples for $T_{C,3}$ was 698 539.397 847 69. From this analysis, we obtained a transit time of $T_{C,3} = 2458\,813.0913 \pm 0.0046$, which is 1.50 ± 0.11 h earlier than predicted. The best-fitting model from this analysis is shown in Fig. 1 and the derived transit time variation is shown in Fig. 2.

Downloaded from https://academic.oup.com/mnrasl/article/504/1/L45/6228864 by guest on 11 December 2024

4 TTV ANALYSIS

Due to its anomalously low density, HIP 41378 f is an attractive target for atmospheric characterization studies. As such, knowing the precise ephemerides for future transits is of high importance. Therefore, we use analytical TTV formulas from Lithwick, Xie & Wu (2012) to predict the times of the upcoming transits of HIP 41378 f, in particular the next two transits in 2021 May and 2022 November.

Of the planets already known in the system, the TTV signal of HIP 41378 f will be most affected by HIP 41378 d and HIP 41378 e. These two planets have masses of $M_{\rm d} < 4.6\,{\rm M}_{\oplus}$ and $M_{\rm e} = 12 \pm 5\,{\rm M}_{\oplus}$ (Santerne et al. 2019), and reside near to 2:1 and 3:2 mean motion resonances with HIP 41378 f, respectively. The amplitude of the TTVs of HIP 41378 f as a result of its interactions with HIP 41378 d and HIP 41378 e will depend strongly on $M_{\rm d}$ and $M_{\rm e}$, respectively. The interactions with HIP 41378 e are likely to dominate the TTV signal of HIP 41378 f since $M_{\rm e} > M_{\rm d}$ (Santerne et al. 2019) and thus we consider solely the TTVs due to interactions between HIP 41378 f and e for the rest of this analysis. We note that neither HIP 41378 d nor HIP 41378 e were robustly detected by Santerne et al. (2019) in HARPS radial velocity measurements, and so they are only able to place loose constraints on the masses and periods of these planets. The constraints on the period of HIP 41378 e are derived from a combination of transit analyses and asteroseismic stellar constraints (Lund et al. 2019; Santerne et al. 2019). Future monitoring of the TTVs of HIP 41378 f will allow us to place tighter independent constraints on the masses and periods of HIP 41378 d and HIP 41378 e.

We use the Lithwick et al. (2012) analytic formulas for TTV signals for planets in a near mean motion resonance to obtain the following equations for the amplitude, V, and superperiod, $P_{\rm ttv}$, for the TTV signal of HIP 41378 f as a result of its interactions with HIP 41378 e. These are

$$V = P_{\rm f} \frac{M_{\rm pl,e}}{3\pi\Delta M_*} \left(-G + \frac{3}{2\Delta} \left(F\, e_{\rm e} + G\, e_{\rm e} \right) \right), \quad (1)$$

$$P_{\rm ttv} = \frac{P_{\rm f}}{3|\Delta|}, \quad (2)$$

where $P_{\rm f}$ is the mean linear orbital period of HIP 41378 f, $M_{\rm pl,\,e}$, and M_* are the masses of HIP 41378 e and HIP 41378, $e_{\rm e}$ and $e_{\rm f}$ are the orbital eccentricities of HIP 41378 e and HIP 41378 f, respectively, and F and G are coefficients given in table 3 of Lithwick et al. (2012). The Δ parameter is the normalized distance to resonance

$$\Delta = \frac{P_{\rm f}}{P_{\rm e}} \frac{2}{3} - 1, \quad (3)$$

where $P_{\rm e} = 369 \pm 10\,{\rm d}$ is the mean linear orbital period of HIP 41378 e,. Using the planetary parameters given in table 1 of Santerne et al. (2019), we calculate values of $V = 1.3667$ d, and $P_{\rm ttv} = 8757.577$ d. We note that the expected TTV signal from HIP 41378 e alone is enough to account for the TTVs observed in Section 2. Additional planets in the system are not required to explain the observations (nor do the observations rule them out).

With just three transit times, we cannot use TTV modelling to place any constraints on the masses and orbital eccentricities of the planets in the HIP 41378 system. Neither can we robustly refine the period of HIP 41378 e. However, we can combine the analytical TTV signals derived in Lithwick et al. (2012) with our knowledge of HIP 41378 f and e to predict the times of the next transits of HIP 41378 f. We do this using an MCMC sampling method, again using EMCEE Ensemble Sampler. The TTV model we use for this sampling is of the form

$$T_{{\rm C},N} = T_0 + P_{\rm f} N + V \sin\left(\frac{2\pi P_{\rm f}}{P_{\rm ttv}} (N + \phi) \right), \quad (4)$$

Table 1. Confidence intervals for the predictions of $T_{\rm C,\,4}$ and $T_{\rm C,\,5}$.

	$T_{\rm C,\,4}$ (BJD TDB–2450000)	$T_{\rm C,\,5}$ (BJD TDB–2450000)
Median (per cent)	9355.087	9897.078
68	9355.064–9355.118	9897.018–9897.192
95	9355.032–9355.156	9896.910–9897.293
99	9355.020–9355.205	9896.884–9897.455

where $T_{{\rm C},N}$ is the time of transit centre of the Nth transit, T_0 is a reference epoch and N is the the transit epoch, such that $T_0 + P_{\rm f}N$ is the mean linear ephemeris of HIP 41378 f, and ϕ is the phase shift of the TTV signal. The free parameters in this sampling are T_0, $P_{\rm f}$, ϕ, $M_{\rm pl,\,e}$, $P_{\rm e}$, $e_{\rm e}$, and $e_{\rm f}$. For the parameters $M_{\rm pl,\,e}$, $P_{\rm e}$, $e_{\rm e}$, and $e_{\rm f}$, we impose Gaussian priors using the posterior values from Santerne et al. (2019). In this way, we explore the parameter space of TTV signals that can explain the transit times we observe for HIP 41378 f and are also physically plausible. For the sampling, we run 40 walkers each for 200 000 steps as a burn-in, and then a following 50 000 steps to explore the parameter space. The resultant predicted TTV signal from this sampling is given in Fig. 2. The median values of the resultant probability distributions for $T_{\rm C,\,4}$ and $T_{\rm C,\,5}$, as well as the 68, 95, and 99 per cent confidence intervals, are provided in Table 1.

5 CONCLUSIONS

We detected a transit of HIP 41378 f on 2019 November 24 and 25, the first ever ground-based transit detection for this planet, primarily with data obtained using NGTS. As this is just the third ever transit of HIP 41378 f detected, we confirm the 542.08-d orbital period of this planet. This long orbital period makes HIP 41378 f the longest period planet to have a transit detected from the ground. The long transit duration (19 h) makes detecting transits of HIP 41378 f challenging and makes photometric efforts with increased longitudinal coverage useful for recovering such transits. On the other hand, the fact that many of the observations taken for this particular effort were not able to be used to constrain the transit parameters highlights the value of photometric facilities like NGTS, when it comes to obtaining high-precision photometry of bright stars like HIP 41378.

We found the transit to arrive 1.50 h earlier than predicted from a linear extrapolation of the *K2* transits (Vanderburg et al. 2016; Becker et al. 2019) and extensive spectroscopic monitoring (Santerne et al. 2019). Using analytic formulas for TTV signals from Lithwick et al. (2012), we have shown that the TTV observed for HIP 41378 f can be explained solely through the interaction between HIP 41378 e and HIP 41378 f. Therefore, the presence of additional planets in the HIP 41378 system is not required to explain our observations. However, our observations do not rule out the presence of additional planets. We predict that the next transit of HIP 41378 f will be centred on BJD 2459355.087 with a 99 per cent confidence interval of 4.4 h (2021 May 20), and the following transit will occur around BJD 2459897.078 with a 99 per cent confidence interval of 13.7 h (2022 November 13).

Both $P_{\rm ttv}$ and V depend strongly on the ratio of $P_{\rm f}/P_{\rm e}$. As $P_{\rm f}$ is well constrained by the available transits of HIP 41378 f, this results in the amplitude and period of the predicted TTV signal depending strongly on the orbital period of HIP 41378 e. The current large uncertainty on $P_{\rm e}$ combined with the shallow transit depth of just 1.5 mmag means

Downloaded from https://academic.oup.com/mnrasl/article/504/1/L45/6228864 by guest on 11 December 2024

that detecting another transit of HIP 41378 e, especially with ground-based facilities, will be tough. However, doing so would greatly refine the predictions of the TTV signal of HIP 41378 f. Additionally, detecting the upcoming transits of HIP 41378 f will allow us to greatly refine the ephemeris of HIP 41378 e, due to the constraints that the improved measurements of V and $P_{\rm ttv}$ will place on $P_{\rm e}$. The next transit of HIP 41378 e is predicted to have a centre time of $T_{\rm C} = 2459\,356 \pm 60$ (UT 2021 May 21). HIP 41378 d is in near 4:3 mean-motion resonance with HIP 41378 e, and so based on our TTV models we expect HIP 41378 d to also experience large TTVs. Therefore, detecting transits of HIP 41378 d will further allow us to refine our TTV models and make better predictions for upcoming transits of HIP 41378 e. Using the sampling method from Section 4, we predict the next transit of HIP 41378 d to have a transit mid-point of $T_{\rm C} = 2459\,393.13 \pm 0.59$ (2021 June 27).

With six planets in the HIP 41378 system, many of which reside near to mean-motion resonances, there are likely to be lots of interactions between the planets. With only a small number of transit detections for each of the outer three planets, a full dynamical analysis of the system is beyond the scope of this work. However, this robust transit detection of HIP 41378 f by NGTS and the discovery of significant TTVs in the system demonstrates that with future photometric monitoring we will be able to characterize the amplitude and super-period of the TTV signal of HIP 41378 f. This monitoring will enable us to place independent constraints on the masses, orbital periods, and eccentricities of the planets in this remarkable system.

ACKNOWLEDGEMENTS

This paper is based on data collected by the NGTS project, the SPECULOOS network, the Asiago Observatory, the Las Cumbres Observatory global telescope network, the MuSCAT2 instrument, the PEST Observatory, the Lick Observatory, the Hazelwood Observatory, the Phillip's Academy Observatory, and the PROMPT-8 telescope at CTIO. For full acknowledgments for these facilities, we refer the reader to the facility papers cited in this paper.

MRK is supported by the NSF Graduate Research Fellowship, grant No. DGE 1339067. DJA acknowledges support from the STFC via an Ernest Rutherford Fellowship (ST/R00384X/1). MNG acknowledges support from MIT's Kavli Institute as a Juan Carlos Torres Fellow. NN is partly supported by JSPS KAKENHI Grant Numbers JP17H04574, JP18H01265, and JP18H05439, and JST PRESTO Grant Number JPMJPR1775, and a University Research Support Grant from the National Astronomical Observatory of Japan (NAOJ). JSJ acknowledges support by FONDECYT grant 1201371, and partial support from CONICYT project Basal AFB-170002.

DATA AVAILABILITY

The NGTS, Asiago, SSO, and SNO photometric data are available in the online supplementary material.

REFERENCES

Agol E., Steffen J., Sari R., Clarkson W., 2005, MNRAS, 359, 567
Barbary K., 2016, J. Open Source Softw., 1, 58
Becker J. C. et al., 2019, AJ, 157, 19
Bertin E., Arnouts S., 1996, A&AS, 117, 393
Bryant E. M. et al., 2020, MNRAS, 494, 5872
Burdanov A., Delrez L., Gillon M., Jehin E., 2018, SPECULOOS Exoplanet Search and Its Prototype on TRAPPIST. Springer International Publishing, Cham
Claret A., Bloemen S., 2011, A&A, 529, A75
Collins K. A. et al., 2018, AJ, 156, 234
Delrez L. et al., 2018, in Marshall H. K., Spyromilio J., eds, Proc. SPIE Conf. Ser. Vol. 10700, Ground-based and Airborne Telescopes VII. SPIE, Bellingham, p. 21
Eastman J., Siverd R., Gaudi B. S., 2010, PASP, 122, 935
Foreman-Mackey D., Hogg D. W., Lang D., Goodman J., 2013, PASP, 125, 306
Gaia Collaboration et al., 2016, A&A, 595, A2
Gaia Collaboration, Brown A. G. A., Vallenari A., Prusti T., de Bruijne J. H. J., Babusiaux C., Bailer-Jones C. A. L., 2018, A&A, 616, 22
Gillon M., 2018, Nat. Astron., 2, 344
Howell S. B. et al., 2014, PASP, 126, 398
Irwin M. J. et al., 2004, in Peter J. Q., Alan B., eds, SPIE Conf. Ser. Vol. 5493, Optimizing Scientific Return for Astronomy through Information Technologies. SPIE, Bellingham, p. 411
Kawahara H., Masuda K., 2019, AJ, 157, 218
Kempton E. M. R. et al., 2018, PASP, 130, 114401
Lithwick Y., Xie J., Wu Y., 2012, ApJ, 761, 122
Lund M. N. et al., 2019, AJ, 158, 248
Murray C. A. et al., 2020, MNRAS, 495, 2446
Nascimbeni V., Piotto G., Bedin L. R., Damasso M., 2011, A&A, 527, A85
Santerne A. et al., 2019, preprint (arXiv:1911.07355)
Sebastian D. et al., 2021, A&A, 645, A100
Smith A. M. S. et al., 2020, Astron. Nachr., 341, 273
Vanderburg A. et al., 2016, ApJ, 827, L10
Wheatley P. J. et al., 2018, MNRAS, 475, 4476

SUPPORTING INFORMATION

Supplementary data are available at *MNRASL* online.

Please note: Oxford University Press is not responsible for the content or functionality of any supporting materials supplied by the authors. Any queries (other than missing material) should be directed to the corresponding author for the article.

[1]*Dept. of Physics, University of Warwick, Gibbet Hill Road, Coventry CV4 7AL, UK*
[2]*Centre for Exoplanets and Habitability, University of Warwick, Gibbet Hill Road, Coventry CV4 7AL, UK*
[3]*Aix Marseille University, CNRS, CNES, LAM, F-13007 Marseille, France*
[4]*INAF – Osservatorio Astronomico di Padova, Vicolo dell'Osservatorio 5, I-35122 Padova, Italy*
[5]*Astrobiology Research Unit, Université de Liège, Allée du 6 Août 19C, B-4000 Liège, Belgium*
[6]*Department of Earth, Atmospheric and Planetary Science, Massachusetts Institute of Technology, 77 Massachusetts Avenue, Cambridge, MA 02139, USA*
[7]*School of Physics and Astronomy, University of Leicester, Leicester LE1 7RH, UK*
[8]*Departamento de Astronomía, Universidad de Chile, Casilla 36-D Santiago, Chile*
[9]*National Astronomical Research Institute of Thailand, 260 Moo 4, Donkaew, Mae Rim, Chiang Mai 50180, Thailand*
[10]*Space Sciences, Technologies and Astrophysics Research (STAR) Institute, Université de Liège, 19C Allèe du 6 Août, B-4000 Liège, Belgium*
[11]*Observatoire Astronomique de l'Université de Genève, Chemin Pegasi 51, CH-1290 Versoix, Switzerland*
[12]*University of Bern, Center for Space and Habitability, Gesellschaftsstrasse 6, CH-3012 Bern, Switzerland*
[13]*Institute of Planetary Research, German Aerospace Center, Rutherford-strasse 2, D-12489 Berlin, Germany*
[14]*Department of Earth and Planetary Science, Graduate School of Science, The University of Tokyo, 7-3-1 Hongo, Bunkyo-ku, Tokyo 113-0033, Japan*

Downloaded from https://academic.oup.com/mnrasl/article/504/1/L45/6228864 by guest on 11 December 2024

[15]*Instituto de Astrofísica de Canarias (IAC), E-38205 La Laguna, Tenerife, Spain*
[16]*Department of Astronomy and Tsinghua Centre for Astrophysics, Tsinghua University, Beijing 100084, China*
[17]*Astrobiology Research Unit, Université de Liège, 19C Allèe du 6 Août, B-4000 Liège, Belgium*
[18]*Perth Exoplanet Survey Telescope (PEST), Perth, Western, Australia*
[19]*Department of Physics, and Kavli Institute for Astrophysics and Space Research, Massachusetts Institute of Technology, Cambridge, MA 02139, USA*
[20]*Department of Earth and Planetary Sciences, University of California, Santa Cruz, CA 95064, USA*
[21]*Centro de Astrofísica y Tecnologías Afines (CATA), Casilla 36-D Santiago, Chile*
[22]*Department of Astronomy and Astrophysics, University of California, Santa Cruz, CA 95064, USA*
[23]*Instituto de Astronomía, Universidad Católica del Norte, Angamos 0610, 1270709 Antofagasta, Chile*
[24]*Astrophysics Group, Cavendish Laboratory, J.J. Thomson Avenue, Cambridge CB3 0HE, UK*
[25]*Komaba Institute for Science, The University of Tokyo, 3-8-1 Komaba, Meguro, Tokyo 153-8902, Japan*
[26]*JST, PRESTO, 3-8-1 Komaba, Meguro, Tokyo 153-8902, Japan*
[27]*Astrobiology Center, 2-21-1 Osawa, Mitaka, Tokyo 181-8588, Japan*
[28]*Phillips Academy Observatory, Phillips Academy, Andover, MA 01810, USA*
[29]*Departamento de Astrofísica, Universidad de La Laguna (ULL), E-38206 La Laguna, Tenerife, Spain*
[30]*School of Physics and Astronomy, University of Birmingham, Edgbaston, Birmingham B15 2TT, UK*
[31]*Hazelwood Observatory, Hazelwood, Australia*

This paper has been typeset from a TEX/LATEX file prepared by the author.

Downloaded from https://academic.oup.com/mnrasl/article/504/1/L45/6228864 by guest on 11 December 2024